

## THERMAL STABLE POROUS CRYSTALS FROM MONTMORILLONITE

## I. Preparation and the properties of Al and Zr pillared montmorillonites

JOZEF KRAJČOVIČ, IVAN HORVÁTH

*Institute of Inorganic Chemistry, Slovak Academy of Sciences, Dúbravská cesta, 842 36 Bratislava*

Received 12. 8. 1991

*Al and Zr pillared clays precursors were prepared by the interaction of the particular inorganic cation nad montmorillonite suspension. Al and Zr pillared montmorillonites were obtained through the calcination of individual precursor at 500° C. The methods of thermal analysis, I. R. spectroscopy, X-ray diffraction and B. E. T. were used to determine the basic properties of these new types of materials. The prepared porous crystals exhibited the specific surface area about 100 m<sup>2</sup> g<sup>-1</sup> stable till up to 700° C.*

## INTRODUCTION

The concept of the clays pillaring reflects the opinions to improve properties of the original clay minerals, the smectites especially. Barrer et al. [1] prepared the bentonites exhibiting favourable diffusion and sorption properties by introducing alkylammonium cations into montmorillonite interlayer space. When the robust inorganic cations are used a precursor is obtained which, after calcination, provides the rise of the metal oxide clusters forming the pillars in the interlayer space of the smectite minerals [2]. The scheme of the pillared clay preparation is in Fig. 1.

Brindley and Semples [3] prepared the first “pillared” smectite with the properties comparable with the commercial zeolites. Later, were these materials used as a molecular sieves, especially. Nowadays the pillared clays are utilized as the catalysts [4, 5], in the crude oil processing [6, 7] and other conversions [8–11]. It is further developed their using as a molecular sieves [12, 13] and they put in the praxis of the construction of clay-modified electrodes [14, 15].

Recently, the properties of the pillared clays were discussed in a review paper [16].

The aim of this work was to prepare a thermal stable porous crystal using a domestic bentonite from

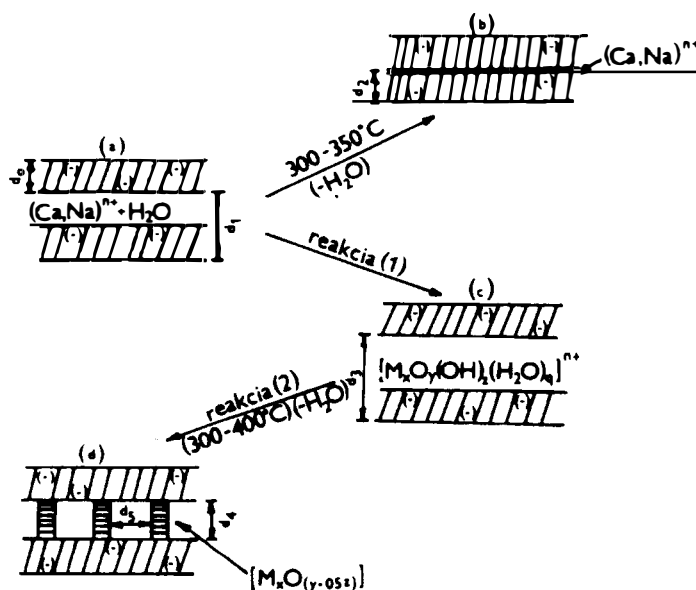


Fig. 1. Scheme of the preparation of the pillared montmorillonite

(a) – the layered structure of montmorillonite (further MMT) with the localization of the negative charge on the layers;  $d_1 = d_{001} = 1.2 - 1.6$  nm depending on the amount of the water molecules layers in MMT interlayer space;  
 (b) – dehydrated layers of MMT (disappearance of the porous structure);  $d_2 = (d_0 + d_{exch.cat}) = 0.96 - 0.98$  nm depending on the size of the exchangeable cation (exch. cat.);  $d_0$  = the height of the MMT elementary unit cell;  
 (c) – the situation after the intercalation (cation exchange) of the hydrated polynuclear inorganic cation;  $d_3 = 1.8 - 2.2$  nm, depending on the conditions of the precursor preparation and the kind of the cation;  
 (d) – the layered structure of the final product after calcination of the precursor (situation c); the height of the pillars formed by oxide clusters  $d_4 = 0.7 - 1.2$  nm;  $d_5$  – the lateral distances between the pillars.

Jelšovský Potok locality and to investigate its properties by the methods of thermal analysis, I. R. spectroscopy and X-ray diffraction.

## EXPERIMENTAL

### The materials

The fraction less than 2  $\mu\text{m}$  from bentonite Jelšovský Potok (Central Slovakia) was used. Montmorillonite content checked by TG and XRD methods was  $90 \pm 5$  wt. %. Montmorillonite was converted to the sodium form using the standard exchange method, dried at 60°C (2 hrs.) and grinded. The chemical composition of the material after sodium saturation: (wt. %)  $\text{SiO}_2$  (63.1),  $\text{Al}_2\text{O}_3$  (20.6),  $\text{Fe}_2\text{O}_3$  (3.1),  $\text{CaO}$  (0.16),  $\text{MgO}$  (3.12),  $\text{Na}_2\text{O}$  (2.83),  $\text{TiO}_2$  (0.18), loss on ignition (6.24).

### Pillaring agents

The hydroxy-aluminium solution containing Al ions was prepared by the titration of 0.2 M  $\text{AlCl}_3$  with 0.2 M  $\text{NaOH}$  solution. The solution of sodium hydroxide was added very slowly at the permanent stirring until the molar ratio  $\text{OH}/\text{Al} = 2.0$  was reached. The obtained hydroxy-aluminium solution was then aged in HT conditions at 97°C (6 hrs.). During this aging the polymerization of aluminium cations is suggested to occur giving rise to the formation of cations:  $[\text{Al}_{13}\text{O}_4(\text{OH})_{24}(\text{H}_2\text{O})_{12}]^{7+}$  [18, 20, 22].

The hydroxy-Zr solution was obtained through hydrolysis of 0.2 M solution of  $\text{ZrOCl}_2$  at 97°C during 24 hrs. It is known, that a crystalline  $\text{ZrOCl}_2 \cdot 8\text{H}_2\text{O}$  compound produces a tetramer cation  $[\text{Zr}_4(\text{OH})_8(\text{H}_2\text{O})_{16}]^{8+}$  in the water and then due to fast hydrolysis the  $[\text{Zr}_4(\text{OH})_{14}(\text{H}_2\text{O})_{10}]^{2+}$  cations are formed. The polymerization of these cations can be influenced changing temperature and the time of the aging as described previously [25].

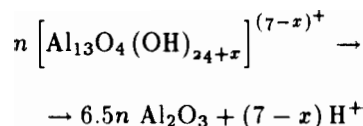
### Precursor preparation

The suspension of Na-montmorillonite containing 1 wt. % of the solid in the deionized water was mixed slowly with the aged pillaring solution at room temperature. The ratio X/clay (where X = Al, Zr) was controlled: 2 mM Al/g montmorillonite (MMT); 10 mM Zr/g MMT. After the exchange reaction and continuous stirring (1 hr.) the intercalated product was separated and washed (using deionized water). Then the sample was dried (at 60°C) and grinded.

### Precursor calcination

The dried samples of precursor were further calcined for 2 hours at 500°C in the air. In the case of Al-precursor the conversion of the complex  $\text{Al}_{13}$

cations to a metal clusters  $\text{Al}_x\text{O}_y$  (forming the permanent pillars in MMT interlayer space) is supposed to proceed according to the equation reported by [17]:



It is evident, that the thermal transformation of precursor results in generation of the protonic acidity of the pillared clay formed during the calcination.

The formation of the Zr oxide pillars occurred similarly by the calcination of Zr-precursor as described in [11].

### The methods

#### Thermal analysis

The thermal analysis of the materials under study was performed using Derivatograph Q-1500 D (MOM Budapest) when the 150 mg samples were heated in Pt pans at the heating rate  $10 \pm 1^\circ\text{C}$  per min in static

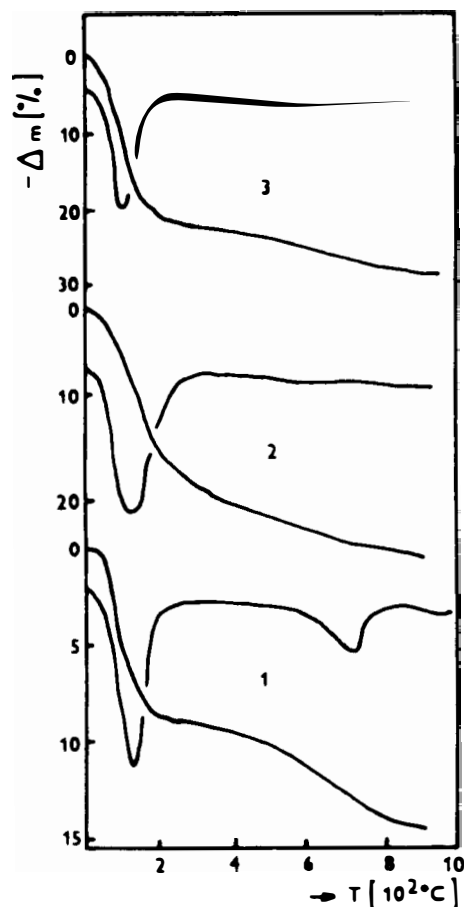


Fig. 2. TG and DTG curves: Na-MMT (1); Al-pillared MMT (2); Zr-pillared MMT (3).

air. The results of thermal analysis are presented in Figs. 2 and 3.

#### I. R. spectroscopy

I. R. absorption spectra were monitored using Perkin Elmer 983 G spectrometer in the range 300–4000  $\text{cm}^{-1}$  from KBr discs (0.3–0.7 mg of the sample +300 mg of KBr). The absorption maxima typical for the MMT structure were evaluated according [21, 26]. I. R. spectra are presented in Figs. 4–6.

#### X-ray diffraction analysis (XRD)

The powder textureless samples were used for XRD measurements using Philips diffractometer PW 1050 ( $\text{CuK}\alpha$  radiation filtered by Ni). The results are in Fig. 7.

#### The specific surface area determination

B.E.T. method using nitrogen adsorption was used for the specific surface area determination.

## RESULTS AND DISCUSSION

### Na-montmorillonite

#### Thermal analysis

Two distinct weight losses occur when Na-MMT is heated according to TG curves in Figs. 1 and 2. The

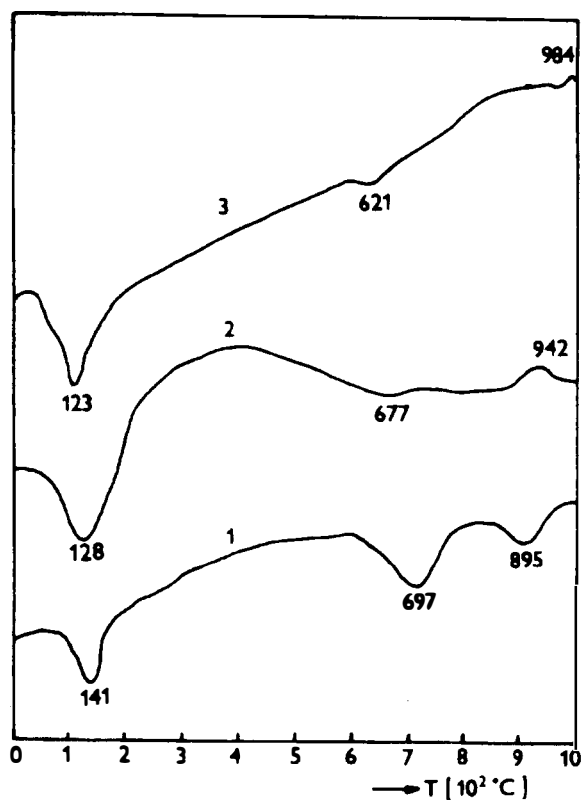


Fig. 3. DTA curves: Na-MMT (1); Al-pillared MMT (2); Zr-pillared MMT (3).

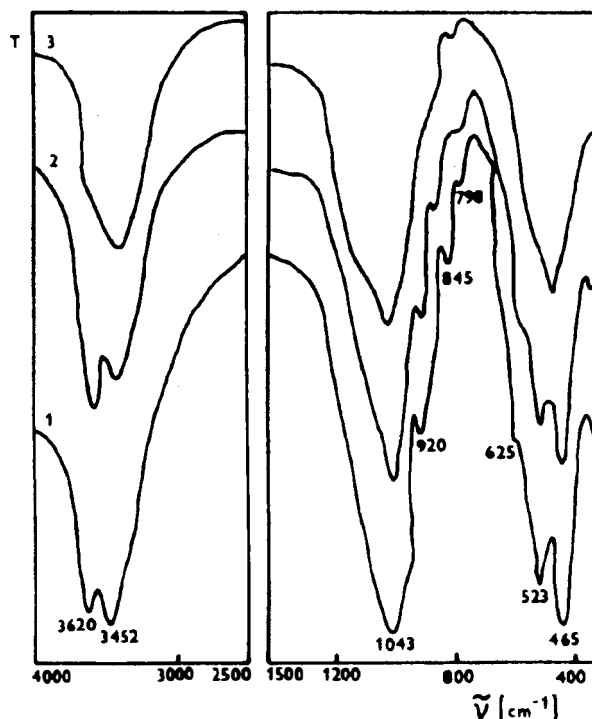


Fig. 4. Infrared spectra: Na-MMT (R. T.) (1), 500°C (2); 700°C (3).

first one belongs to the dehydration when the water from the interlayer space is released. This process is indicated by endothermic peak at 141°C in DTA curve (Fig. 3, curve 1). The second weight loss indicated by TG represents dehydroxylation of the MMT structure with endothermic reaction in DTA curve with DTA peak at 697°C. Next DTA curve deviations (e.g. a slight endothermic peak at 895°C as well as a implication of the exothermic change in the temperature region 900–1000°C) can be ascribed to the MMT structure decomposition and to the formation of a new high-temperature phases.

#### I. R. spectroscopy

The absorption maxima at 3620  $\text{cm}^{-1}$  (Fig. 4) reflects the stretching vibrations of the structural OH groups of MMT. This band is partially covered with an intensive band belonging to a molecular water (at 3452  $\text{cm}^{-1}$ ) which is present in the interlayer space of MMT as well as in a KBr discs. The intensity of this band decreases when the sample is heated.

The stretching vibration of Si-O groups in tetrahedral part of MMT structure is indicated by absorption band at 1043  $\text{cm}^{-1}$ . This is the most intensive band in the whole spectra. The band at 920  $\text{cm}^{-1}$  belongs to the bending vibrations of AlAlOH and the band at 845  $\text{cm}^{-1}$  represents the bending vibrations of Al-MgOH groups. The band at 798  $\text{cm}^{-1}$  indicates the vibration of Si-O groups present in amorphous  $\text{SiO}_2$

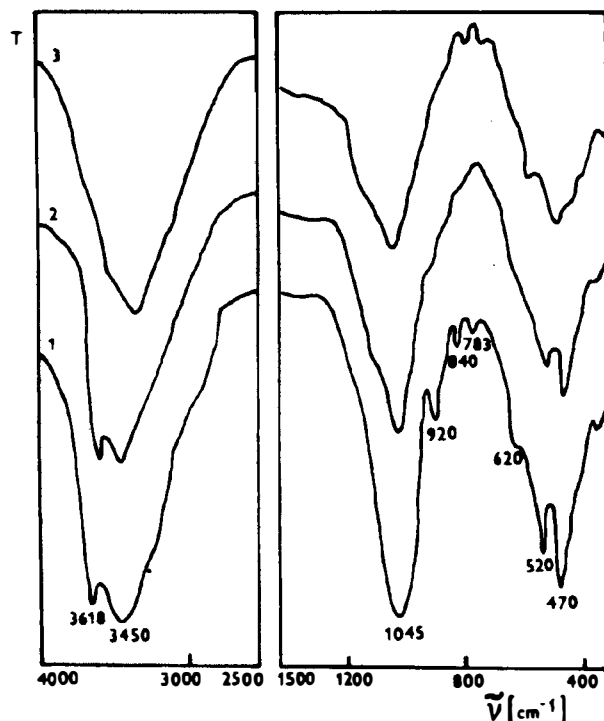


Fig. 5. Infrared spectra: Al-pillared MMT (R. T.) (1); 500°C (2); 700°C (3).

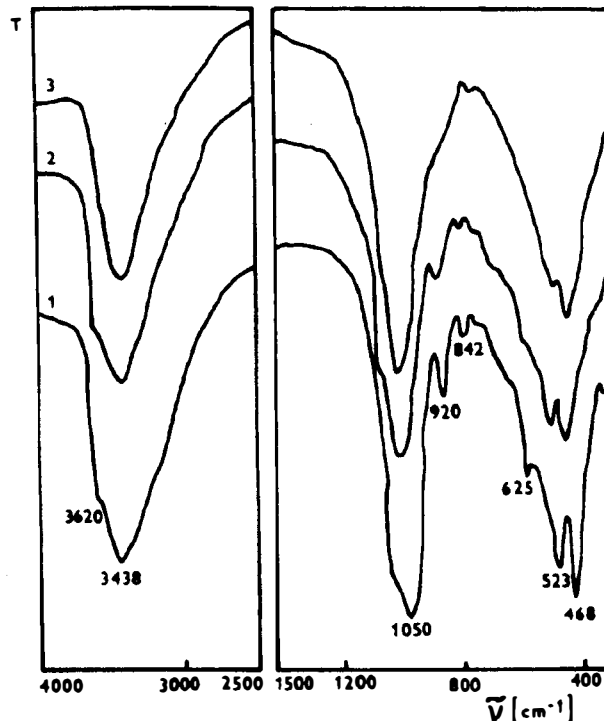


Fig. 6. Infrared spectra: Zr-pillared MMT (R. T.) (1); 300°C (2); 500°C (3).

admixture present in bentonite. The vibrations of R-O-R (R = Al, Mg) indicates the band at 625  $\text{cm}^{-1}$ . The bands at 523  $\text{cm}^{-1}$  and 465  $\text{cm}^{-1}$  belong to the bending vibrations of Si-O-Al and Si-O-Si groups, respectively.

The bending vibrations of OH groups decreases in the intensity when MMT sample is heated. The gradual disappearing of absorption bands belonging to the R-O-R vibrations (625  $\text{cm}^{-1}$ ) and to the Si-O-Al vibrations (520  $\text{cm}^{-1}$ ) indicates the decomposition of the octahedral sheet in MMT structure on the heating (Fig. 4, curve 3).

#### XRD measurements

The XRD traces of Na-MMT before and after heating are shown in Fig. 7. The  $d_{001}$  spacing of the non-heated sample 1.27 nm corresponds to the interlayer distance 0.26 nm. The heating of the sample at 500°C results in dehydration of the interlayer space and the collapsing of  $d_{001}$  value to 0.94 nm. This is a proof of a low thermal stability of Na-MMT sample.

#### Al-pillared montmorillonite

##### Thermal measurements

The introducing of a robust  $[\text{Al}_{13}\text{O}_4(\text{OH})_{24}(\text{H}_2\text{O})_{12}]^{7+}$  cations into a MMT interlayer is connected with further endothermic reactions on heating because of dehydroxylation and dehydration of the

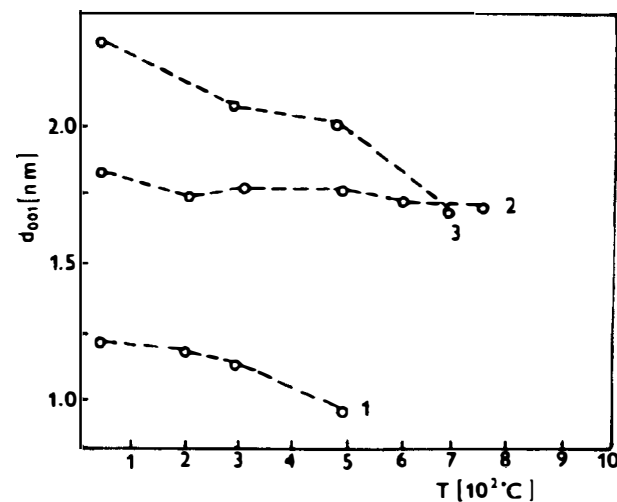


Fig. 7. Temperature dependence of  $d_{001}$  spacings: 1 - Na-MMT; 2 - Al-Pillared MMT; 3 - Zr-pillared MMT.

oxy-hydroxy aluminium cation. There is only one dehydration step on the TG curve of Al-pillared MMT precursor (Fig. 2, curve 2). The dehydration and dehydroxylation processes are not significantly separated as distinct from nontreated Na-MMT sample.

The endothermic peak at 128°C on DTA curve (Fig. 3, curve 2) represents the whole dehydration

process of the Al-pillared MMT precursor sample. The dehydration starts earlier in comparison with nontreated Na-MMT. As distinct from TG curve is it possible to observe a slight endothermic peak in DTA curve at 677°C belonging to dehydroxylation of the MMT structure. The formation of high temperature phases indicates exothermic peak at 942°C.

#### I. R. spectroscopic measurements

There are not any significant differences in spectra of non-treated Na-MMT, Al-precursor (at room temperature) and Al-pillared MMT (after heating at 500°C) (Fig. 5). It is possible to observe only a gradual disappearing of the stretching vibration bands of OH groups in the spectra of the Al-pillared MMT sample. The introducing of the robust Al polynuclear cation into MMT interlayer did not change the spectra of Al-precursor and/or Al-pillared MMT samples. There are only small differences in the ratios of intensities of absorption in the region of Si-O bending vibrations at 520 and 470  $\text{cm}^{-1}$  when Na-MMT, Al-precursor and Al-pillared MMT samples are compared (decreasing of intensity of the absorption band at 520  $\text{cm}^{-1}$  in the case of the Al-pillared MMT sample).

#### X-ray diffraction measurements

The temperature dependences of the  $d_{001}$  spacing for Al-precursor and Al-pillared MMT are shown in Fig. 7. It is evident, that the  $d_{001}$  value for non-treated Na-MMT increased from 1.22 nm to 1.83 after intercalation of the Al-polynuclear cation (when Al-precursor was formed) and then slightly decreased by reaching 1.77 nm value after heating of precursor at 500°C. The  $d_{001}$  value 1.77 nm remains stable till up to 700°C which gives the evidence that was prepared the porous crystal containing thermal stable openings with an average diameter of 0.81 nm.

#### Zr-pillared montmorillonite

##### Thermal measurements

Zr-precursor in heating releases the water in two stages: at first there occurs the dehydration process when the molecular water is removed from the both of the MMT interlayer and the coordination sphere of Zr polynuclear cation. In this stage of dehydration proceeds the dehydroxylation of Zr cations as well. Dehydroxylation of the MMT structure is represented by the second weight loss at higher temperatures according to the TG curve in Fig. 2. Both of these processes are characterized as endothermic peaks of DTA curve at 123°C and 621°C, respectively (Fig. 3, curve 3).

Moreover, the DTA curve shows an exothermic peak at 984°C reflecting the formation of the high temperature phases.

#### The I. R. spectroscopic results

Zr-precursor and Zr-pillared MMT exhibit the similar I. R. spectra as nontreated Na-MMT (the same situation as for Al varieties). The shoulder at 3620  $\text{cm}^{-1}$  in the spectra of Zr-precursor (Fig. 6, pattern 1) is associated with the stretching vibration of OH groups. This band is not present in the spectra of Zr-pillared MMT (Fig. 6, pattern 3). The band in the region of 1050  $\text{cm}^{-1}$  associated with Si-O stretching vibrations becomes less broad on heating. The typical vibration bands of the MMT structure at 920, 842 and 625  $\text{cm}^{-1}$  present in the spectra of the Zr-precursor disappear after calcination. Similarly, it is possible to observe the lower relative intensity of the absorption band at 525  $\text{cm}^{-1}$  (Si-O-Al vibrations) in the spectra of Zr-pillared MMT sample (Fig. 6, pattern 3).

#### X-ray diffraction measurements

There are two pronounced maxima in the XRD patterns of Zr-precursor sample at 2.32 and 1.22 nm associated with  $d_{001}$  and  $d_{002}$  spacings (Fig. 7). These data prove the introducing of the robust zirconium cations into MMT interlayer. Furthermore, XRD measurements of Zr-precursor sample after calcination at 500°C revealed the  $d_{001}$  spacing of 2.02 nm. Accordingly, the thermal stable porous crystal with the two-dimensional porous structure containing the pores with the diameter of 1.06 nm was prepared.

The specific surface area determination using B. E. T. adsorption method the following data on the specific surface area were determined: Na-MMT = 37  $\text{m}^2\text{g}^{-1}$ , Al-pillared MMT = 129  $\text{m}^2\text{g}^{-1}$  and Zr-pillared MMT = 150  $\text{m}^2\text{g}^{-1}$ .

#### CONCLUSIONS

The results showed that montmorillonite Jelšovský Potok (Central Slovakia) is suitable for the production of a new type porous crystals. By introducing of pillaring agents of a type  $[\text{M}_x\text{O}_y(\text{OH})_z(\text{H}_2\text{O})_q]_{\text{aq}}^{n+}$  into montmorillonite interlayer a small inorganic cations are exchanged and the pillared montmorillonite precursor is formed. Then, after calcination the formation of the metal oxide clusters occurs keeping the montmorillonite layers apart till up to temperature 700°C. Accordingly, the thermal stable pillared montmorillonites were prepared with the pores opening of 0.81 (M = Al) and/or 1.06 nm (M = Zr) and with the specific surface area exceeded 100  $\text{m}^2\text{g}^{-1}$ .

## TERMICKY STABILNÉ PÓROVITÉ KRYŠTÁLY NA BÁZE MONTMORILLONITU.

### I. Príprava a vlastnosti Al a Zr pilierovaných montmorillonitov.

JOZEF KRAJČOVIČ, IVAN HORVÁTH

Ústav anorganickej chémie SAV,  
Dúbravská cesta 9, 842 36 Bratislava

Interkaláciu Na montmorillonitu Al a Zr polykationmi typu  $[Al_{13}O_4(OH)_{24}(H_2O)_{12}]^{7+}$  a  $[Zr_4(OH)_8(H_2O)_{16}]^{8+}$  sa pripravili prekuzory. Vlastnosti prekuzorov boli študované metódami termickej analýzy, infračervenej spektroskopie, BET adsorpcie a RTG difrakčnej analýzy. Po kalcinácii boli generované Al a Zr oxidové klastre, ktoré držia od seba montmorillonitové vrstvy až do 700°C, výsledkom čoho bol vznik termicky stabilných pórovitých kryštálov s veľkosťou pórov 0,8 (Al), 1,2 (Zr) nm a merným povrchom okolo 100 m<sup>2</sup>.g<sup>-1</sup>.

Obr. 1. Schéma prípravy pilierovaného montmorillonitu.

(a) - vrstevnatá štruktúra montmorillonitu (Ďalej MMT) so symbolickým vyznačením záporného náboja na vrstvách;  $d_1 = d_{001}$  a podľa množstva molekúl vody dosahuje hodnoty 1,2-1,6 nm;

(b) - MMT po dehydratácii (zánik pórovitej štruktúry);  $d_2 = d_0 + d_{vk(deh.)} = 0,96-0,98$  nm, podľa veľkosti dehydratovaného vymeniteľného kationu (vk);  $d_0$  - výška trojvrstvia základnej jednotky štruktúry MMT;

(c) - situácia po interkalácii (kationovej výmene) hydratovaného ozihydroxy kationu;  $d_3 = 1,8-2,2$  nm, podľa podmienok reakcie kalcinácie a druhu kationu;

(d) - vrstevnatá štruktúra finálneho produktu po kalcinácii komplexu c; výška piliera oxidového klastru  $d_4 = 0,7-1,2$  nm;  $d_5$  - vzdialenosť medzi piliermi.

Obr. 2. TG krivky a DTG krivky Na MMT (1), Al PILL MMT (2), Zr PILL MMT (3).

Obr. 3 DTA krivky Na MMT (1), AL PILL MMT (2), Zr PILL MMT (3).

Obr. 4. IČ spektrum Na MMT pri RT (1), 500°C (2), 700°C (3).

Obr. 5. IČ spektrum Al PILL MMT pri RT (1), 500°C (2), 700°C (3).

Obr. 6. IČ spektrum Zr PILL MMT pri RT (1), 300°C (2), 500°C (3).

Obr. 7. Závislosť parametra  $d_{001}$  skúmaných vzoriek od teploty: 1 Na MMT, 2 Al PILL MMT, 3 Zr PILL MMT.